

OPTIMIZATION OF CONTINUOUS ETHANOL PRODUCTION FROM SPENT BLACK TEA HYDROLYSATE USING IMMOBILISED *ESCHERICHIA COLI* KO11

MEHMET KALENDER and HAMDI SONER ALTUNDOĞAN

Department of Bioengineering, Firat University, 23100, Elazığ, Turkey

✉ *Corresponding author: M. Kalender, mkalender@firat.edu.tr*

Received January 10, 2025

Spent black tea waste (SBTW) was subjected to acid and then enzymatic hydrolyses. Fermentation experiments were carried out in a continuous fermentation system (CFS) and were optimized by RSM. Independent variables in RSM were as follows: reduced sugar concentration, flow rate, temperature, and immobilised cell fill ratio. The response variable was bioethanol yield. The SBTW hydrolysate was composed of fermentable sugars, such as glucose, xylose, galactose, and arabinose. It was determined that the significant single parameters in the developed model were reduced sugar concentration and flow rate. A bioethanol yield above 90% was achieved at the optimal point and this yield value continued steadily for 192 h. The dilution rate, hydraulic retention time, productivity, CO₂%, and pH range at the optimal point were 0.300 h⁻¹, 3.333 h, 41.698 g/L day, 81.40%, and 5.81-6.5, respectively. The outer surface of the beads, with an average diameter of 1.871 mm, was smooth, and the *E. coli* KO11 cells on the inner surface of the beads were rod-shaped, as typical of these bacteria.

Keywords: continuous bioethanol production, spent black tea, acidic and enzymatic hydrolysis, immobilised *E. coli* KO11, optimization

INTRODUCTION

Clean and reliable energy sources have become very important in today's world because of environmental problems associated with pollution, such as global warming, climate change, acid rain, as well as depleting fossil fuel reserves.¹ Thus, in developed and developing countries, some precautions are taken to overcome associated challenges or difficulties. A recent example of this is the European Green Deal, which set an important goal – to achieve zero greenhouse gas emissions by 2050.²

Renewable energy sources, which are a good alternative to fossil fuels, can be classified as hydro power, biomass, geothermal, solar energy, and wind energy.³ Biomass energy (11%) is the third most used renewable energy type, after the wind (43%) and the solar energy (40%).^{3,4} It can be used for heat and power generation, and as transportation fuel in energy conversion systems or applications. It is suitable for some small-scale applications, like cooking and lighting,⁴ but it is also commonly converted to biofuels (bioethanol, biobutanol, biodiesel, biogas, biohydrogen, bio-oil

etc.) to produce renewable energy. According to the OECD report, it is predicted that the use of biofuels in global transportation will reach between 15-23% by 2050.⁵ Biofuels used in transportation are commonly bioethanol and biodiesel. Bioethanol and gasoline blends or pure bioethanol are suitable as fuel for vehicles.⁶ E10 known as “gasohol” is a standard fuel containing 10% bioethanol and 90% gasoline.¹ It is reported that global bioethanol production has reached approximately 30 billion gallons in 2019.⁷ Unlike other biofuels, bioethanol is also used as a disinfectant in many fields, especially in the field of healthcare,⁸ confirming its value as a chemical agent.

Bioethanol production methods depend on the type of raw biomass material used in fermentation. These methods can be generally classified as first generation (sugar-containing feedstocks), second generation (lignocellulosic biomass), and third generation (algal biomass).⁹ Sugar-containing materials used in the fermentation processes have the food-versus-fuel debate problem. This leads to

limitations in using sugar based feedstocks to produce bioethanol. Many studies have been intensively focused on bioethanol production from lignocellulosic and algal biomasses, which are good alternatives to the first generation bioethanol feedstock.^{10,11} Lignocellulosic biomass is a substantial renewable substrate in bioethanol production due to the generally non-edible and abundant supply.¹² Lignocellulosic feedstocks used in second generation bioethanol production are generally agricultural residues.^{13,14} Other lignocellulosic sources include dedicated energy crops, forestry by-products, industrial residues, municipal wastes, roadside hay *etc.*¹⁵⁻¹⁷

Due to their composition, including cellulose, hemicelluloses, and lignin, lignocellulosic biomasses must be subjected to some pretreatment and hydrolysis processes before fermentation. In order to be metabolized by microorganisms used in bioethanol production, cellulose and hemicelluloses must be converted to simple sugars (galactose, xylose, arabinose, glucose, mannose, fucose and others, depending on the raw material). Common applied hydrolysis techniques for fermentable sugars from lignocellulosic substrates are acidic and enzymatic hydrolyses.^{1,18} The acidic hydrolysis is considered the oldest and most commonly used method to hydrolyse lignocellulosic materials due to being a simple technique, which does not require thermal energy, and effectively hydrolyses hemicelluloses. However, in acidic hydrolysis, toxic inhibitors might be produced (*e.g.* furfural, 5-HMF, and phenolic compounds, some organic acids), leading to some limitations in the fermentation stage.¹⁹⁻²¹ Thus, a detoxification treatment is carried out to remove these inhibitors after acidic hydrolysis.²² Enzymatic hydrolysis offers several advantages, such as high sugar yield, low temperature and pH conditions, simultaneous operation with bioethanol production and low toxic by-product formation. However, it is an expensive technique. Additionally, undesired interaction with lignin and prolonged hydrolysis time are its main limitations.²³ Thus, this study aims to improve the fermentable sugar production from lignocellulosic

feedstock by sequentially using acidic and enzymatic hydrolysis.

Bioethanol is produced using the obtained hydrolysates and microorganisms. *Saccharomyces cerevisiae*, *Zymomonas mobilis*²⁴ and recombinant *Escherichia coli* strains are commonly used in bioethanol production. Recombinant *E. coli* KO11 can metabolise simultaneously both hexoses and pentose sugars.²⁵

The fermentation for bioethanol production can be conducted in batch, semi-batch, and continuous systems. In the batch bioreactor, the long fermentation time and the need for pre- and post-process sterilization are important limitations.²⁶ A disadvantage of semi-batch bioethanol production is that the culture volume in the bioreactor is not maintained constant. The continuous bioethanol production is carried out in the exponential phase of microorganism growth. There are continuous input and output streams in continuous bioreactors. Thus, culture volume, cell number, the product and substrate concentrations, and some physical parameters, such as pH, temperature, and dissolved oxygen concentration, are maintained as approximately constant during the fermentation process.²⁷

Tea leaves (*Camellia sinensis*) contain polyphenols, cellulose and hemicelluloses (holocellulose), enzymes, vitamins, lignin, minerals, lipids, and proteins.²⁸⁻³⁰ Turkey is an important black tea producer country and is the first in the world in terms of per capita black tea consumption. Black tea production and consumption per person in Turkey are tabulated in Table 1 between 2019 and 2023.³¹ This beverage is prepared using hot water extraction.³² After the extraction, spent black tea waste (SBTW) is generated and it contains remarkable holocellulose contents. This study considers using this waste as a feedstock in bioethanol production.

According to the authors' knowledge, there is no study on the production of bioethanol from tea waste in a continuous system. In this study, the optimization of bioethanol production from SBTW, using immobilised recombinant *E. coli* KO11, has been investigated in a continuous fermentation system (CFS).

Table 1
Statistical data of total tea production and consumption in Turkey between 2019 and 2023

	2019	2020	2021	2022	2023
Production (thousand tons)	1.480	1.407	1.450	1.454	1.270
Consumption per person (kg)	15	14.6	15.2	14.5	12.5

EXPERIMENTAL

Materials

Experimental studies were carried out using SBTW samples supplied from the tea room of Firat University Bioengineering Department in Turkey. SBTW samples were washed three times with distilled water, dried at 25 °C, milled, sieved (-30+50 mesh), and kept in sealed glass jars. Some physical properties and chemical compositions of SBTW samples were close those of a previous paper.³³ Thus, the moisture of SBTW was measured as 5.87% (w/w). Lignin, cellulose, hemicellulose and extractive matter contents of SBTW were 37.22% (w/w), 21.15% (w/w), 23.31 (w/w), and 13.07 (w/w), respectively.

Hydrolysis of SBTW samples

The SBTW samples were subjected to diluted acid hydrolysis with sulphuric acid and then enzymatic hydrolysis.

Acid hydrolysis

The acid hydrolysis conditions (55 g/L solid concentration, 1.4% (v/v) acid concentration, 120 min, and 125 °C) were close to those used in a previous article.³³ A detoxification treatment was carried out to remove especially phenolic compounds, which may have formed during acidic hydrolysis and are known to affect adversely bioethanol production.²² Based on this approach, the alkali detoxification treatment proposed by İmamoğlu and Sukan was performed.³⁴

Enzymatic hydrolysis

After acidic hydrolysis and detoxification, enzymatic hydrolysis was performed to convert the residual holocellulose in SBTW. The reason for this is the decrease in enzymatic performance due to interactions with lignin or lignin-carbohydrate complexes (LCCs).³⁵ The SBTW hydrolysate obtained from acid hydrolysis and detoxification treatments was centrifuged. The supernatant was reserved for fermentation studies, while the precipitate was used for enzymatic hydrolysis. The hydrolysis was conducted using Cellic® CTec3 HS (Novozymes), a multi-enzyme cocktail (4 g enzyme/100 g cellulose), at 150 rpm, in 0.05 M sodium citrate buffer (pH 4.8), at 50 °C for 72 hours.³⁶ The enzyme cocktail includes AA9 molecules (lytic polysaccharide monooxygenases), β -glucosidases, and hemicellulases.

Bacterial cultures

Recombinant *E. coli* KO11 (ATCC® 55124™) was used in fermentation experiments. This microorganism was grown in modified Luria-Bertani (LB) liquid medium containing glucose 20 g/L (Merck), bacteriological peptone 10 g/L (Lab M), yeast extract 5 g/L (Biolife), NaCl 5 g/L (Merck), and chloramphenicol (0.6 g/L) at 37 °C, 100 rpm and for 24 h. The culture

medium was stored in cryotubes containing 20% (v/v) glycerol at -80 °C for use in next experiments.

Immobilization of recombinant *E. coli* KO11 cells

Immobilization experiments of bacterial cultures were carried out in a sterile laminar flow cabinet with sterilized solutions at 121 °C for 15 min. Activated bacterial cultures at the end of 16-hour incubation period were centrifuged at 4100 rpm for 5 min. A cell suspension in sterilised water was prepared using the centrifugation pellet. The cell suspension and 2% (w/v) sodium alginate solution were mixed in a beaker. Then, the mixture was slowly dropped using a single-use syringe into a gently stirred 2.5% (w/v) CaCl₂ solution. Calcium alginate beads were formed by solidifying upon contact with CaCl₂ and then were incubated to cross-link and stabilize for 30 min in the same solution. To remove un-immobilised cells and excess Ca²⁺ ion, the beads were washed in a 0.9% (w/v) NaCl solution.

CFS experiments and optimization

The bioethanol production experiments were carried out using CFS, as illustrated in Figure 1. The main apparatus of the CFS experimental setup consisted of a borosilicate glass column, with the diameter of 3 cm and the length of 15 cm, a feed reservoir, circulating water bath (Miprolab, Turkey), peristaltic pumps (Watson Marlow, UK), and product reservoir. The column was indirectly heated with a heating jacket that allows hot water circulation. Air filter and air lock were used to create an anaerobic atmosphere in CFS. Before the fermentation experiments, all parts of CFS and SBTW hydrolysate were autoclaved at 121 °C for 15 min. Except for glucose, the modified Luria-Bertani (LB) medium components used in recombinant *E. coli* KO11 growth were added to the SBTW hydrolysate. The pH of the hydrolysate was adjusted to 6.5. The hydrolysate was transferred to the CFS column containing the immobilised recombinant *E. coli* KO11 beads.

The bioethanol yield from the SBTW hydrolysate in CFS was optimized using the response surface methodology of central composite design (RSM-CCD), with four factors (reduced sugar concentration g/L, the flow rate in CFS mL/min, column temperature °C, and immobilised cell fill ratio w/v %) and surface centred. Table 2 tabulates the levels of the independent variables in CCD for CFS experiments. The 30 runs of CCD for CFS experiments were given in Table 3.

The response variable of CCD was selected as bioethanol yield, given in Equation (1):

$$\text{Bioethanol yield (\%)} = \left(\frac{c_{s,max}}{(c_{s,in} - c_{s,max})y_e} \right) 100\% \quad (1)$$

where $c_{s,in}$ – inlet reduced sugar concentration of CFS column (the independent variable in Table 2, $c_{s,max}$ – CFS effluent reduced sugar concentration at the maximum produced bioethanol concentration, y_e – theoretical ethanol yield for hexoses and pentoses (0.511 g ethanol/g 5 or 6-carbon sugars).³⁷ According to

Table 3, an experimental run of bioethanol production from SBTW using *E. coli* KO11 in CFS was performed in the volume of 100 mL and for 48 h. Liquid and gas samples were taken from CFS at different time points to

measure the pH and concentrations of ethanol, reducing sugar, and CO₂. Also, an experiment was carried out for ten days under the optimum conditions determined.

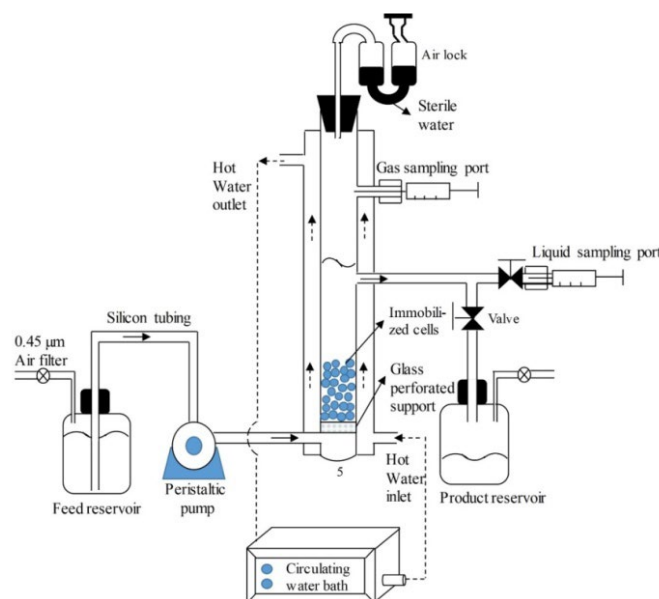


Figure 1: Experimental set-up for bioethanol production from SBTW using immobilised recombinant *E. coli* KO11 in CFS

Table 2
Symbols and related levels of the independent variables at RSM-CCD for CFS experiments

Symbol	Independent variables	- α	-1	0	+1	+ α
A	Inlet reduced sugar concentration (g/L)	20.00	35	50.00	65.00	80.00
B	Flow rate (mL/min)	0.00	0.25	0.50	0.75	1.00
C	Temperature (°C)	30.00	31.75	33.50	35.25	37.00
D	Immobilised cell fill ratio (% w/v)	25.00	37.50	50.00	62.50	75.00

Analytical methods

Sugar analyses

Total reducing and fermentable (5 and 6-carbon) sugar concentrations of the culture media for *E. coli* KO11 during fermentation experiments were measured using 3,5-dinitrosalicylic acid (DNS),³⁸ and by the high pressure liquid chromatography (HPLC) method.³³ The DNS experiments were performed using a Shimadzu-1800 UV-Visible Spectrophotometer at 570 nm. HPLC analyses were carried out using a Shimadzu LC-20AT, equipped with a CARBOSep CHO-682 (Transgenomic) column and a refractive index detector (RID). Before HPLC measurements, the samples to be analysed were filtered through 0.45 µm pore size polytetrafluoroethylene (PTFE) syringe filters (Sartorius) and then subjected to HPLC analysis. The carrier phase was ultra-pure water. The column oven temperature and carrier flow rate were 80 °C and 0.4 mL/min, respectively. The sugar standards were prepared using sucrose (Carlo Erba), arabinose (Sigma-

Aldrich), xylose (Sigma-Aldrich), mannose (TSI), galactose (Sigma-Aldrich), and glucose (Merck).

Alcohol analyses

The concentrations of bioethanol produced from SBTW in the CFS were analysed using the gas chromatography (GC) technique. The GC analyses were performed on a Shimadzu GC2010Plus with FID detector. The column, the carrier gas (nitrogen) flow rate, injection port temperature, the oven temperature, and detector temperature of GC were BP20 capillary column (0.25 mm ID, 0.25 µm thickness, 30 m length), 0.91 mL/min, 200 °C, 140 °C, and 250 °C, respectively. The injection volume was 1 µL, and the sample was passed through 0.45 µm pore size PTFE syringe filters before GC analysis. Ethanol (Merck) was used to prepare calibration standard solutions.

Scanning electron microscopy (SEM)

SEM images of raw SBTW, hydrolysed (acidic and enzymatic) SBTW samples, and immobilised cell beads were taken with a Zeiss EVO MA 10 device at an

acceleration voltage of 15 kV. The bacteria to be scanned by SEM were fixed in 0.1 M pH 6.5-7.0

phosphate-buffer saline (PBS) fixative 2.5% glutaraldehyde at room temperature for 2 h.³⁹

Table 3
Design matrix created from RSM-CCD for CFS experiments

Experiment number	Inlet reduced sugar concentration (g/L)	Flow rate (mL/min)	Temperature (°C)	Immobilised cell fill ratio (% w/v)
1	35	0.25	31.75	37.50
2	65	0.25	31.75	37.50
3	35	0.75	31.75	37.50
4	65	0.75	31.75	37.50
5	35	0.25	35.25	37.50
6	65	0.25	35.25	37.50
7	35	0.75	35.25	37.50
8	65	0.75	35.25	37.50
9	35	0.25	31.75	62.50
10	65	0.25	31.75	62.50
11	35	0.75	31.75	62.50
12	65	0.75	31.75	62.50
13	35	0.25	35.25	62.50
14	65	0.25	35.25	62.50
15	35	0.75	35.25	62.50
16	65	0.75	35.25	62.50
17	20	0.50	33.50	50.00
18	80	0.50	33.50	50.00
19	50	0.00	33.50	50.00
20	50	1.00	33.50	50.00
21	50	0.50	30.00	50.00
22	50	0.50	37.00	50.00
23	50	0.50	33.50	25.00
24	50	0.50	33.50	75.00
25	50	0.50	33.50	50.00
26	50	0.50	33.50	50.00
27	50	0.50	33.50	50.00
28	50	0.50	33.50	50.00
29	50	0.50	33.50	50.00
30	50	0.50	33.50	50.00

CO₂ analyses

Fermentative CO₂ production yield from SBTW in the CFS was determined using GC (Thermo Scientific TRACE 1300) equipped with a thermal conductivity detector (TCD). A capillary column TG-BOND Q (Thermo Scientific, USA; 30 m × 0.32 mm × 10.0 µm) was used. The carrier gas was helium and the injection volume was 0.5 mL. The temperatures of the oven, injection port, and detector were 50 °C, 120 °C, and 200 °C, respectively.

RESULTS AND DISCUSSION

Hydrolysis results and SEM images of SBTW

After acidic and enzymatic hydrolyses of SBTW were carried out under experimental conditions given in the previous section, its total reduced sugar content was measured as 20.102 g/L

and 23.096 g/L, respectively. HPLC results showed that 5 and 6 carbon fermentable sugars content of the SBTW hydrolysate obtained from acidic and enzymatic hydrolyses were glucose (3.303 g/L), xylose (1.896 g/L), galactose (3.198 g/L), and arabinose (3.175 g/L). It is seen that the fermentable sugar content of SBTW corresponds to approximately 50% of the total reducing sugar content. The sugar content of SBTW given above is similar to research findings of previous studies.^{40,41}

SEM images of SBTW samples, recorded before and after hydrolysis, are shown in Figure 2 (a-c) in this study. The results presented in Figure 2 (a-b) clearly indicate that the cell wall structure of SBTW was modified due to the degradation of lignin and hemicelluloses during the acidic hydrolysis.⁴² As shown in Figure 2 (c), the

structural degradation appears to progress further during enzymatic hydrolysis. The relatively lower impact of enzymatic hydrolysis, compared to

acidic hydrolysis, is an expected outcome and aligns well with previous reports in the literature.⁴³

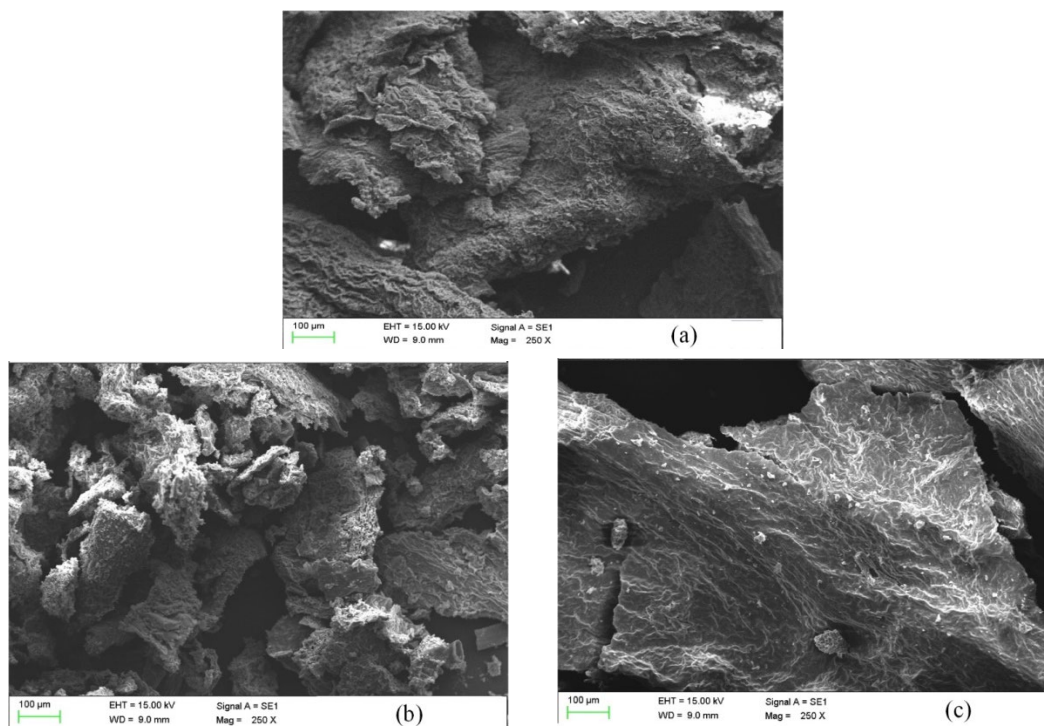


Figure 2: SEM images of SBTW before and after acid and enzymatic hydrolyses: (a) raw, (b) after acid hydrolysis, (c) after enzymatic hydrolysis

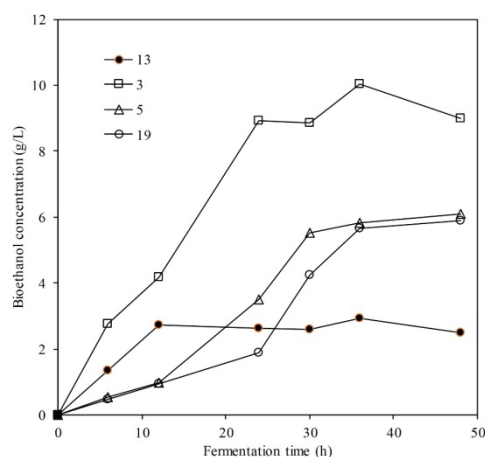


Figure 3: Fermentation time vs bioethanol concentration graph for specified runs of CCD

Results of CFS experiment and optimization

Changes of bioethanol concentration in CFS medium as a function of fermentation time during the four working runs (3, 5, 13, and 19) given in Table 3 are shown in Figure 3. As seen in Figure 3, the bioethanol concentration increases with increasing time up to 30 h, and remained constant after that. A similar result for other experimental runs given in Table 3 was also observed. Thus, the

maximum bioethanol concentration was calculated for a fermentation time of 30 h.

In the present study, RSM-CCD was applied to optimize the fermentation conditions, and obtain a correlation for the bioethanol yield and the variables: reduced sugar concentration, flow rate, column temperature, and immobilised cell fill ratio. In the optimization studies given in Table 3, a set of 30 experiments were performed with 6

replications at the central point (zero level). Regression analyses were conducted fitting four models (linear, 2FI, quadratic, and cubic) using Design Expert. The most appropriate model was the quadratic model, with an F-value of 33.28 and a p-value of <0.0001. The analysis of variance (ANOVA) results of the quadratic model for bioethanol production from SBTW in CFS are given in Table 4. The F-value of 25.96 and the p-value Prob>F less than 0.05 in Table 4 indicate that the proposed model is significant. It can be said that the model has a good fit because of the low standard deviation and high R^2 values. As seen in ANOVA results in Table 4, the value Adeq. Precision meaning the signal/noise ratio was obtained as 27.780. If this value is greater than 4, the model is sufficient. Thus, there is an adequate signal of the proposed model in the design space navigation. The difference between Adj. R^2 (0.886) and Pred. R^2 (0.763) is $0.123 < 0.2$. This means that Pred. R^2 is in agreement with Adj. R^2 . A mathematical expression of bioethanol yield in terms of actual factors generated the Design Expert program, except for the non-significant parameters in the model, is as follows:

$$\text{Bioethanol Yield (\%)} = -317.945 + 0.448 A - 374.855 B + 11.489 C + 11.958 D - 2.069 A B + 21.088 B C - 0.449 C D - 206.273 B^2 + 0.030 D^2$$

where the units of the independent variables are as given in Tables 2 and 3.

The residuals defined as the difference between actual and predicted values can be also used in the

ANOVA test.⁴⁴ A chart of normal plot of residuals and a graph of residuals-run number created using RSM-CCD were illustrated in Figure 4. As seen Figure 4 (a), a normal distribution of errors for bioethanol production yield was obtained since the residuals vary linearly with the normal % probability. From Figure 4 (b), the graph of residuals versus run number for bioethanol production from SBTW in CFS exhibits a random distribution between -3.6595 and +3.6595. This means that the proposed model is reliable, adequate, with no violation of constant variance assumption.

From the ANOVA test given in Table 4, it was noted that the significant model terms were A, B, AB, BC, CD, B^2 , and D^2 due to p-values less than 0.05. However, there was no effect of temperature, cell fill ratio, quadratic terms of the reduced sugar concentration and temperature, binary interactions for AC, AD, and BD on the proposed model because of p-values greater than 0.05. 3D graphs showing binary interactions of independent variables can be obtained using RSM-CCD. Such graphs and the perturbation plot obtained using the developed model for significant interactions (AB, BC, and CD) are depicted in Figure 5 (a-d).

Figure 5 (a) shows that the bioethanol production increases up to the flow rate of approximately 0.5 mL/min (equal to the dilution rate of 0.3 h^{-1} and the hydraulic retention time of 3.333 h) and decreases slightly after this flow rate value at low reduced sugar concentrations.

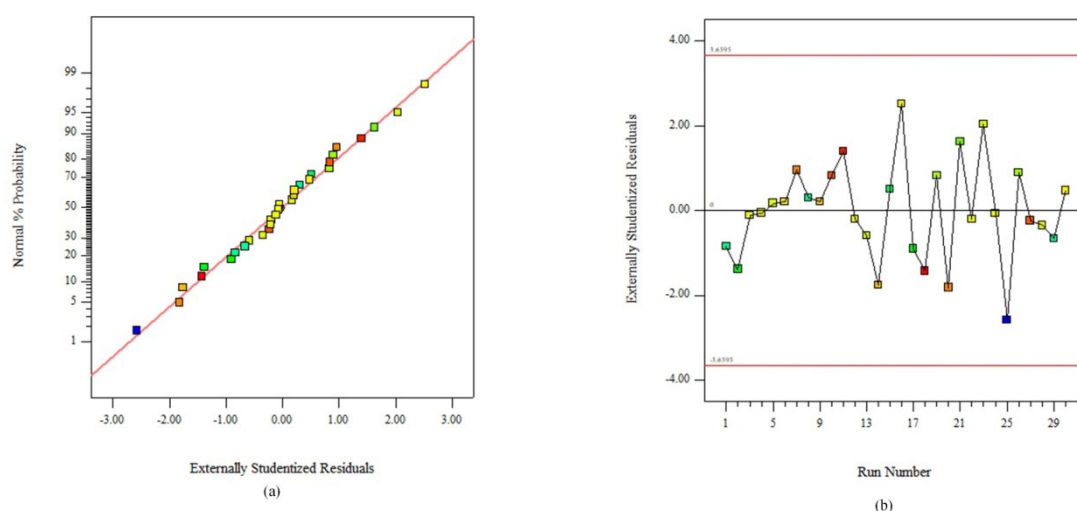


Figure 4: Externally studentized residuals vs run number (a) and normal probability against externally studentized residuals (b) graphs created using RSM-CCD for bioethanol production from SBTW in CFS

Table 4

ANOVA results of the quadratic model for bioethanol production from SBTW using immobilised *E. coli* KO11 in CFS

Source	Sum of squares	Mean square	F-value	p-value Prob>F	significant
Model	12290.85	1365.65	25.96	<0.0001	
A-Reduced sugar concentration	1861.32	1861.32	35.38	<0.0001	
B-Flow rate	716.82	716.82	13.63	0.0014	
C-Temperature	12.55	12.55	0.24	0.6305	
D-Immobilised cell fill ratio	11.36	11.36	0.22	0.6471	
AB	963.29	963.29	18.31	0.0004	
BC	1361.89	1361.89	25.89	<0.0001	
CD	1543.06	1543.06	29.33	<0.0001	
B ²	4727.60	4727.60	89.87	<0.0001	
D ²	635.80	52.60	12.09	0.0024	
Std. Dev. = 7.250, R ² = 0.921, Adj. R ² = 0.886, Pred. R ² = 0.763, Adeq. Precision = 22.780					

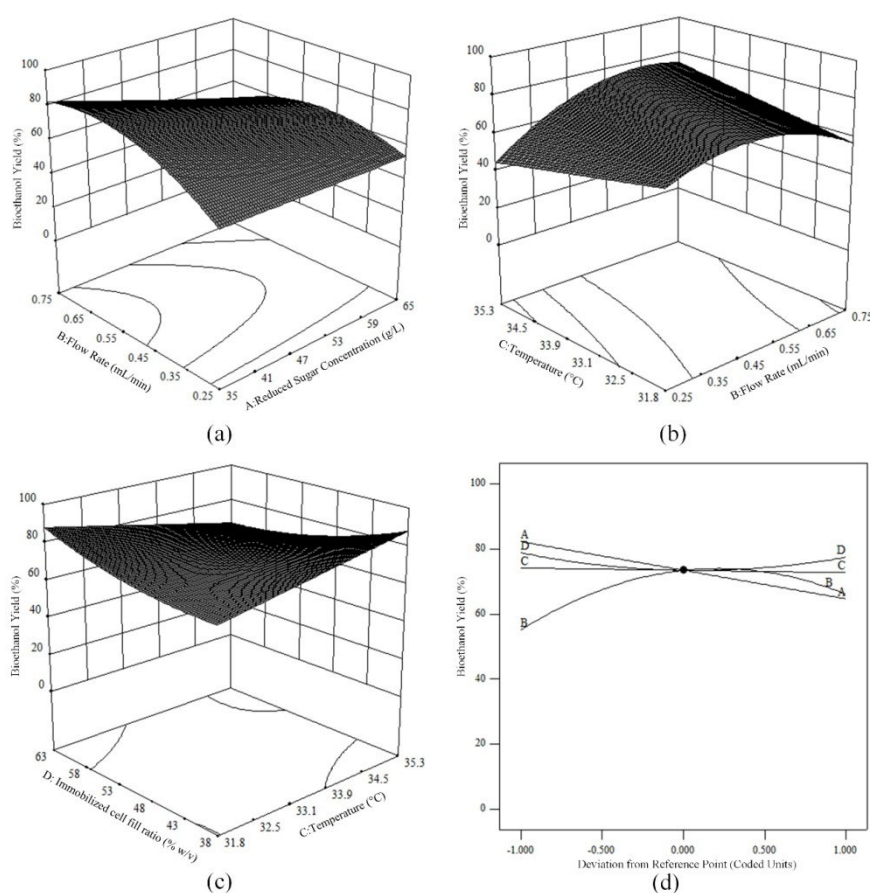


Figure 5: 3D graphs (reduced sugar concentration–flow rate (a), temperature–flow rate (b), immobilised cell fill ratio–temperature (c) and perturbation plot (d) created using RSM-CCD for SBTW bioethanol production in CFS

From the binary interaction between the temperature and the flow rate (Fig. 5 (b)), an optimum point of bioethanol yield was obtained at the flow rate of 0.5 mL/min. Mathew *et al.* investigated the bioethanol production from oilseed rape straw using immobilised *S. cerevisiae* cells in a continuous process.⁴⁵ They found that the produced bioethanol concentration (g/L) decreases as the dilution rate (h^{-1}), which is the ratio of

volumetric flow rate to constant working volume, increases in the range from 0.25 to 1 h^{-1} (corresponding to the hydraulic retention time of 1–4 h). Ghorbany *et al.* obtained a similar result for continuous bioethanol production from cane molasses using immobilised *S. cerevisiae* cells in a hydraulic retention time ranging between 5–15 h.⁴⁶ Karagöz and Özkan⁴⁷ examined ethanol production from wheat straw using a single or co-culture of *S.*

cerevisiae and *Scheffersomyces stipites* in a batch and a continuous system. They indicated that the bioethanol yield (%) slightly increased with increasing the column flow rate at 0.5-1 mL/min (dilution rate in the range of 0.17-0.33 h⁻¹ or hydraulic retention time in the range of 3-6 h). We also observed an increasing bioethanol production yield (%) up to the dilution rate of 0.3 h⁻¹. It is thought that this increase, which is in agreement with the literature, was due to strong mass transfer limitations occurring at very low column flow rate.

As seen in Figure 5 (a), the bioethanol yields at high flow rates and reduced sugar concentrations are lower than those at low flow rates and reduced sugar concentrations. A reason for this situation at high flow rates is the low hydraulic retention time in the continuous fermentation column. Another reason also may be the possible effect of repression caused by higher reduced sugar amounts. A similar result in the bioethanol production from glucose supplemented LB broth using the *E. coli* KO11 (pLOI 1910) strain was found in a previous article.⁴⁸ From Figure 5 (b and c), it is understood that there is almost no effect of temperature on the bioethanol production. Figure 5 (c) shows that the bioethanol production had almost no changes with the immobilised cell fill ratio at low temperatures, but slightly increased with decreasing cell fill ratio at high temperatures. A perturbation plot, which can be used to compare the effects of all the independent variables in the RSM analyses, is presented in Figure 5 (d). The plot shows there are effects of the reduced sugar concentration and flow rate on bioethanol yield, while there is almost no effect of temperature and immobilised cell fill ratio. This result is in agreement with the p-values in the ANOVA table (Table 4). The optimal points

to obtain maximum bioethanol production yield from SBTW used in this study proposed by RSM were 35 g/L reduced sugar concentration, 0.50 mL/min column flow rate, 31.75 °C temperature and 62.50% immobilized cell fill ratio. The bioethanol production yield %, which is the response variable, was approximately 96%, with 0.974 desirability under the optimum conditions.

Experimental validation of RSM

The optimum conditions obtained from RSM were validated by an experimental study carried out in the CFS. The validation experiment was carried out during 192 h. Changes in the produced bioethanol and consumed fermentable sugar concentrations with fermentation time in CFS, under optimum experimental conditions, are shown in Figure 6. As seen in Figure 6, the produced bioethanol concentration firstly increases with increasing fermentation time and then remains constant. On the contrary, the fermentable sugar concentration firstly decreases with increasing time and then approaches the horizontal axis.

Figure 7 illustrates changes of the bioethanol production yield from SBTW calculated using Equation (1), fermentative CO₂%, and pH with time under optimum experimental conditions in CFS.

From Figure 7, it can be said that the bioethanol and fermentative CO₂ productions from SBTW using *E. coli* KO11 in CFS has reached a steady state at the 30th hour. The average values of bioethanol production yields and CO₂% in the steady state in Figure 7 were calculated as 92.970% and 81.40%, respectively.

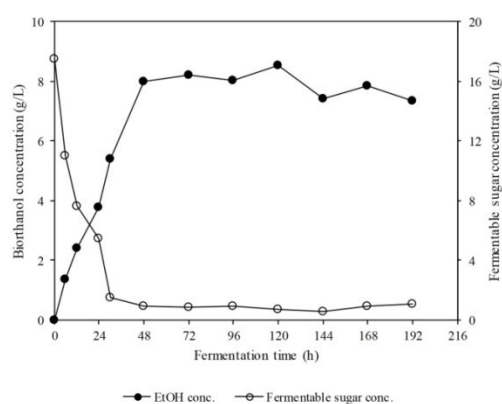


Figure 6: Bioethanol and consumed fermentable sugar concentrations vs fermentation time for bioethanol production from SBTW in CFS

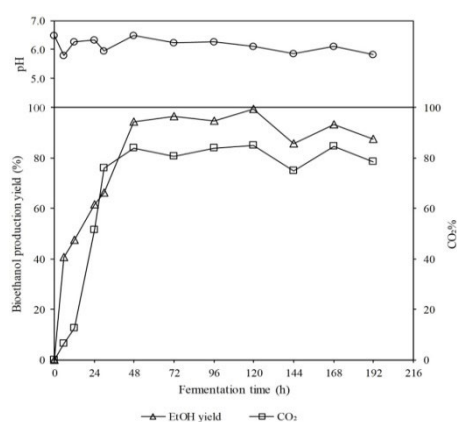


Figure 7: Bioethanol yield and fermentative CO₂ vs fermentation time for bioethanol production from SBTW in CFS

Table 5

Bioethanol yields obtained from various carbon sources using different microorganisms and fermentation operating modes as reported in previous studies and in this work

Carbon source	Microorganism	Operating mode	Maximum EtOH yield (%)	References
Rice hulls and cotton stalks	<i>E. coli</i> KO11	Batch	80.981-86.274	34
LB (glucose and xylose)	<i>E. coli</i> KO11	Batch	72.941-83.332	51
Waste house wood	<i>E. coli</i> KO11	Batch	82.191	52
Mixed sugars (arabinose, glucose and xylose)	<i>E. coli</i> KO11	Batch	90.196-92.157	53
Spent black tea waste	<i>E. coli</i> KO11	Batch	82.745	33
Date palm	<i>Saccharomyces cerevisiae</i> X19G2		94.117	54
Waste glycerol	<i>E. aerogenes</i> ATCC 29007	Continuous	96.000	55
Sugarcane molasses	<i>S. cerevisiae</i>	Continuous	90.469	46
Sugarcane molasses	<i>S. cerevisiae</i> HAU-1	Continuous	95.011	56
Wheat straw	<i>S. cerevisiae</i> and <i>S. stipites</i> co-culture	Continuous	94.579	47
Blackstrap molasses	Immobilized yeast cells on thin-shell silk cocoons	Continuous	92.890	50
Spent black tea waste	<i>E. coli</i> KO11	Continuous	92.970	This study

Table 6

Kinetic parameters for bioethanol production from SBTW using immobilized *E. coli* KO11 in CFS at steady state (after 30 h) under optimum production conditions (35 g/L reduced sugar concentration, 0.50 mL/min column flow rate, 31.75 °C temperature and 62.50% immobilized cell fill ratio)

Initial fermentable sugar (g/L)	Residual sugar fermentable (g/L)	Dilution rate (h ⁻¹)	Hydraulic retention time (h)	Produced alcohol (g/L)	Bioethanol yield (%)	Productivity (g/L day)
17.500	0.850	0.300	3.333	5.790	92.970	41.698

This means that the deviation between the validation value and the predicted (96%) values at the optimum point proposed by RSM is within 3.157%, which is a good fit. The bioethanol production yields obtained from various materials using different microorganisms and fermentation operating modes were compared in Table 5. It is noted that the bioethanol production yield from SBTW in the CFS in this work is at a high level (above 90%), compared to other previous studies. Figure 7 also shows that the pH of the fermentation broth in CFS varied between 5.81 and 6.5, in which *E. coli* KO11 functions efficiently (5.8-7.5).⁴⁹

Some kinetic parameters of the bioethanol production from SBTW in CFS were calculated and presented in Table 6. The yields and

productivity values for bioethanol production in this work were in agreement with the previous studies carried out to produce bioethanol from various lignocellulosic materials.^{47,50}

SEM images of the immobilized recombinant *E. coli* KO11 beads used in ethanol production from SBTW in CFS were illustrated in Figure 8 (a-d). Figure 8 (a) shows that the average diameter of the beads obtained is 1.871 mm. From Figure 8 (b), it is shown that the outer surface of the beads is smooth. Figure 8 (c and d) clearly reveals recombinant *E. coli* KO11 cells on the inner surface of the beads. It may be noted that typical rod-shaped *E. coli* KO11 cells are present, as expected.

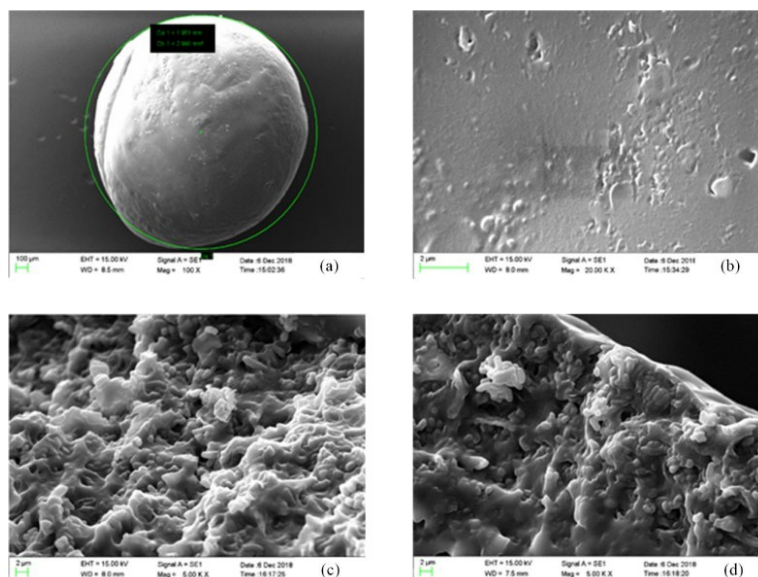


Figure 8: SEM images of immobilized *E. coli* KO11 beads used in ethanol production from SBTW in CFS, (a) immobilised bead, (b) outer surface of the bead, (c) and (d) inner surface of the bead

CONCLUSION

In this work, bioethanol production from SBTW using immobilized recombinant *E. coli* KO11 in CFS was investigated. SBTW samples were subjected to acid and enzymatic hydrolyses, and the hydrolysate consisting of *E. coli* KO11 fermentable sugars, such as glucose, xylose, galactose, and arabinose, was obtained. Optimization results of bioethanol production from SBTW in CFS showed that the significant terms in the model developed using RSM-CCD were A (reduced sugar concentration), B (flow rate), AB, BC, CD, B², and D² (immobilised cell fill ratio). Optimal experimental conditions were the following: 35 g/L reduced sugar concentration, 0.50 mL/min column flow rate, 31.75 °C temperature and 62.50% immobilized cell fill ratio. Bioethanol yields proposed by RSM and obtained from the validation experiment performed under the optimal conditions were 96% and 92.970%, respectively. The CO₂ percentage yield produced by the fermentation carried out at the optimal point was 81.40%. Initial fermentable and residual fermentable sugar concentrations were 17.500 g/L and 0.850 g/L at the optimal experimental point. The dilution rate, hydraulic retention time, and productivity were 0.300 h⁻¹, 3.333 h, and 41.698 g/L per day, respectively. The mean diameter of the spherical immobilised cell beads was measured as 1.871 mm using SEM images. It was observed that the outer surface of the beads was smooth. From the SEM images of the inner surface of the beads, the shape of the recombinant *E. coli* KO11 cells was typical rod-shaped.

ACKNOWLEDGEMENTS: The authors acknowledge the financial support of the Project grant No. 116Y397 made available by Scientific and Technological Research Council of Turkey (TUBITAK).

REFERENCES

- ¹ M. Balat, H. Balat and C. Öz, *Prog. Energ. Combust. Sci.*, **34**, 551 (2008), <https://doi.org/10.1016/j.pecs.2007.11.001>
- ² European Commission, the European Green Deal, https://ec.europa.eu/info/strategy/priorities-2019-2024/european-green-deal_en. Accessed 14.05.2025
- ³ D. Chettri, B. Sharma, S. Singh, A. K. Verma and A. K. Verma, in "Bio-Clean Energy Technologies", edited by P. Chowdhary, N. Khanna, S. Pandit and R. Kumar, Springer, 2022, volume 1, p. 31, https://doi.org/10.1007/978-981-16-8090-8_2
- ⁴ L. Amjith and B. Bavanish, *Chemosphere*, **293**, 133579 (2022), <https://doi.org/10.1016/j.chemosphere.2022.133579>
- ⁵ A. Piwowar and M. Dzikuc, *Energies*, **15**, 2582 (2022), <https://doi.org/10.3390/en15072582>
- ⁶ J. M. de Medeiros Dantas, J.-B. Beigbeder, J. R. G. Cardozo and J. M. Lavoie, *Biomass Bioenerg.*, **169**, 106655 (2023), <https://doi.org/10.1016/j.biombioe.2022.106655>
- ⁷ L. A. J. Letti, E. B. Sydney, J. C. de Carvalho, L. P. de Souza Vandenberghe, S. G. Karp *et al.*, in "Biomass, Biofuels, Biochemicals", edited by I. S. Thakur, A. Pandey, H. H. Ngo, C. R. Soccol, C. Larroche, Elsevier, 2022, p. 373, <https://doi.org/10.1016/B978-0-12-823500-3.00006-6>

- ⁸ K. A. Reynolds, J. D. Sexton, T. Pivo, K. Humphrey, R. A. Leslie *et al.*, *Am. J. Infect. Control*, **47**, 128 (2019), <https://doi.org/10.1016/j.ajic.2018.06.017>
- ⁹ S. M. D. Tavva, A. Deshpande, S. R. Durbha, V. A. R. Palakollu, A. U. Goparaju *et al.*, *Renew Energ.*, **86**, 1317 (2016), <https://doi.org/10.1016/j.renene.2015.09.074>
- ¹⁰ R. Harun and M. K. Danquah, *Process Biochem.*, **46**, 304 (2011), <https://doi.org/10.1016/j.procbio.2010.08.027>
- ¹¹ S. Bhushan, U. Jayakrishnan, B. Shree, P. Bhatt, S. Eshkabilov *et al.*, *J. Environ. Chem. Eng.*, **11**, 109870 (2023), <https://doi.org/10.1016/j.jece.2023.109870>
- ¹² M. Nazar, L. Xu, M. W. Ullah, J. M. Moradian, Y. Wang *et al.*, *J. Clean. Prod.*, **360**, 132171 (2022), <https://doi.org/10.1016/j.jclepro.2022.132171>
- ¹³ N. Singh, M. S. Taggar, J. Kaur, A. Kalia and T. Garg, *Cellulose Chem. Technol.*, **57**, 359 (2023), <https://doi.org/10.35812/CelluloseChemTechnol.2023.57.31>
- ¹⁴ M. Galić, M. Stajić and J. Čilerdžić, *Cellulose Chem. Technol.*, **58**, 1075 (2024), <https://doi.org/10.35812/CelluloseChemTechnol.2024.58.92>
- ¹⁵ J. K. Saini, R. Saini and L. Tewari, *3 Biotech*, **5**, 337 (2015), <https://doi.org/10.1007/s13205-014-0246-5>
- ¹⁶ J. S. Tumuluru, C. T. Wright, R. D. Boardman, N. A. Yancey and S. Sokhansanj, *Am. Soc. Agric. Biol. Eng.*, **2011**, 1 (2011), <https://doi.org/10.13031/2013.37191>
- ¹⁷ N. Rubab, M. Ghazanfar, S. Adnan, I. Ahmad, H. A. Shakir *et al.*, *Cellulose Chem. Technol.*, **57**, 345 (2023), <https://doi.org/10.35812/CelluloseChemTechnol.2023.57.30>
- ¹⁸ P. Lenihan, A. Orozco, E. O'Neill, M. Ahmad, D. Rooney *et al.*, *Chem. Eng. J.*, **156**, 395 (2010), <https://doi.org/10.1016/j.cej.2009.10.061>
- ¹⁹ N. Akhtar, K. Gupta, D. Goyal and A. Goyal, *Environ. Progress Sustain. Energ.*, **35**, 489 (2016), <https://doi.org/10.1002/ep.12257>
- ²⁰ R. Sindhu, P. Binod, E. Gnansounou, T. P. Prabisha, L. Thomas *et al.*, *Indian J. Experiment. Biol.*, **56**, 479 (2018)
- ²¹ M. J. Taherzadeh and K. Karimi, *Int. J. Mol. Sci.*, **9**, 1621 (2008), <https://doi.org/10.3390/ijms9091621>
- ²² S. Larsson, A. Reimann, N.-O. Nilvebrant and L. J. Jönsson, *Appl. Biochem. Biotechnol.*, **77**, 91 (1999), <https://doi.org/10.1385/ABAB:77:1-3:91>
- ²³ Y. Sun and J. Cheng, *Bioresour. Technol.*, **83**, 1 (2002), [https://doi.org/10.1016/S0960-8524\(01\)00212-7](https://doi.org/10.1016/S0960-8524(01)00212-7)
- ²⁴ K. Zhang, X. Lu, Y. Li, X. Jiang, L. Liu *et al.*, *Appl. Biochem. Biotechnol.*, **103**, 2087 (2019), <https://doi.org/10.1007/s00253-019-09620-6>
- ²⁵ D. Chiaramonti, M. Prussi, S. Ferrero, L. Oriani, P. Ottonello *et al.*, *Biomass Bioenerg.*, **46**, 25 (2012), <https://doi.org/10.1016/j.biombioe.2012.04.020>
- ²⁶ I. L. Pepper, C. P. Gerba, T. J. Gentry and R. M. Maier, "Environmental Microbiology", Academic Press, 2011
- ²⁷ B. McNeil and L. Harvey, "Practical Fermentation Technology", John Wiley & Sons, 2008
- ²⁸ S. Guo, M. K. Awasthi, Y. Wang and P. Xu, *Bioresour. Technol.*, **338**, 125530 (2021), <https://doi.org/10.1016/j.biortech.2021.125530>
- ²⁹ G. Lai, Y. Cui, D. Granato, M. Wen, Z. Han *et al.*, *Food Res. Int.*, **155**, 111041 (2022), <https://doi.org/10.1016/j.foodres.2022.111041>
- ³⁰ H. Chen, Z. Qu, L. Fu, P. Dong and X. Zhang, *J. Food Sci.*, **74**, C469 (2009), <https://doi.org/10.1111/j.1750-3841.2009.01231.x>
- ³¹ H. Erkal, Tea Crop Report 2024, <<https://arastirma.tarimorman.gov.tr/tepage>>, Accessed 14.05.2025
- ³² A. Polat, Z. Kalcıoğlu and N. Müezzinoğlu, *Int. J. Gastron. Food Sci.*, **29**, 100559 (2022), <https://doi.org/10.1016/j.ijgfs.2022.100559>
- ³³ A. Yazıcıoğlu and M. Kalender, *Environ. Eng. Manag. J. (EEMJ)*, **21**, (2022)
- ³⁴ E. Imamoglu and F. V. Sukan, *Fuel*, **134**, 477 (2014), <https://doi.org/10.1016/j.fuel.2014.05.087>
- ³⁵ A. Berlin, M. Balakshin, N. Gilkes, J. Kadla, V. Maximenko *et al.*, *J. Biotechnol.*, **125**, 198 (2006), <https://doi.org/10.1016/j.jbiotec.2006.02.021>
- ³⁶ T. A. L. Silva, H. D. Z. Zamora, L. H. R. Varão, N. S. Prado, M. A. Baffi *et al.*, *Waste Biomass Valoriz.*, **9**, 2191 (2018), <https://doi.org/10.1007/s12649-017-9989-7>
- ³⁷ M. Gulati, K. Kohlmann, M. R. Ladisch, R. Hespell and R. J. Bothast, *Bioresour. Technol.*, **58**, 253 (1996), [https://doi.org/10.1016/S0960-8524\(96\)00108-3](https://doi.org/10.1016/S0960-8524(96)00108-3)
- ³⁸ G. L. Miller, *Anal. Chem.*, **31**, 426 (1959), <https://doi.org/10.1021/ac60147a030>
- ³⁹ M. Kaláb, A.-F. Yang and D. Chabot, *Infocus Magazine*, **10**, 42 (2008)
- ⁴⁰ C. T. Scoparo, L. M. Souza, N. Dartora, G. L. Sasaki, A. P. Santana-Filho *et al.*, *Int. J. Biol. Macromol.*, **86**, 772 (2016), <https://doi.org/10.1016/j.ijbiomac.2016.02.017>
- ⁴¹ J. Xiao, J. Huo, H. Jiang and F. Yang, *Int. J. Biol. Macromol.*, **49**, 1143 (2011), <https://doi.org/10.1016/j.ijbiomac.2011.09.013>
- ⁴² S. Sharma, V. Sharma and A. Kuila, *3 Biotech*, **6**, 1 (2016) <https://doi.org/10.1007/s13205-016-0465-z>
- ⁴³ W. Liu, W. Chen, Q. Hou, S. Wang and F. Liu, *RSC Adv.*, **8**, 10207 (2018), <https://doi.org/10.1039/C7RA12732D>
- ⁴⁴ J. Shafaghat and A. Ghaemi, *Iranian J. Sci. Technol. Transac. A: Sci.*, **45**, 899 (2021), <https://doi.org/10.1007/s40995-021-01075-7>
- ⁴⁵ A. K. Mathew, M. Crook, K. Chaney and A. C. Humphries, *Bioresour. Technol.*, **154**, 248 (2014), <https://doi.org/10.1016/j.biortech.2013.12.044>
- ⁴⁶ F. Ghorbani, H. Younesi, A. E. Sari and G. Najafpour, *Renew Energ.*, **36**, 503 (2011), <https://doi.org/10.1016/j.renene.2010.07.016>

- ⁴⁷ P. Karagöz and M. Özkan, *Bioresour. Technol.*, **158**, 286 (2014), <https://doi.org/10.1016/j.biortech.2014.02.022>
- ⁴⁸ I. Deniz, E. Imamoğlu and F. V. Sukan, in *Procs. GreInSus'14*, İzmir, May 8-10, 2014, p. 61
- ⁴⁹ M. Moniruzzaman, S. York and L. Ingram, *J. Ind. Microbiol. Biotechnol.*, **20**, 281 (1998), <https://doi.org/10.1038/sj.jim.2900524>
- ⁵⁰ A. Rattanapan, S. Limtong and M. Phisalaphong, *Appl. Energ.*, **88**, 4400 (2011), <https://doi.org/10.1016/j.apenergy.2011.05.020>
- ⁵¹ L. Yomano, S. York and L. Ingram, *J. Ind. Microbiol. Biotechnol.*, **20**, 132 (1998), <https://doi.org/10.1038/sj.jim.2900496>
- ⁵² N. Okuda, K. Ninomiya, M. Takao, Y. Katakura and S. Shioya, *J. Biosci. Bioeng.*, **103**, 350 (2007), <https://doi.org/10.1263/jbb.103.350>
- ⁵³ B. S. Dien, R. B. Hespell, H. A. Wyckoff and R. J. Bothast, *Enzyme Microb. Technol.*, **23**, 366 (1998), [https://doi.org/10.1016/S0141-0229\(98\)00064-7](https://doi.org/10.1016/S0141-0229(98)00064-7)
- ⁵⁴ I. B. Atitallah, F. Arous, I. Louati, H. Zouari-Mechichi, M. Brysch-Herzberg *et al.*, *Process Biochem.*, **105**, 102 (2021), <https://doi.org/10.1016/j.procbio.2021.03.019>
- ⁵⁵ S. J. Lee, J. H. Lee, X. Yang, H. Y. Yoo, S. O. Han *et al.*, *J. Clean. Prod.*, **161**, 757 (2017), <https://doi.org/10.1016/j.jclepro.2017.05.170>
- ⁵⁶ A. Sheoran, B. Yadav, P. Nigam and D. Singh, *J. Basic Microbiol.*, **38**, 123 (1998), [https://doi.org/10.1002/\(SICI\)1521-4028\(199805\)38:2<123::AID-JOBM123>3.0.CO;2-9](https://doi.org/10.1002/(SICI)1521-4028(199805)38:2<123::AID-JOBM123>3.0.CO;2-9)